Asia-Pacific Journal of Science and Technology: Volume: 29. Issue: 05. Article ID.: APST-29-05-06. Research Article

APST

Asia-Pacific Journal of Science and Technology

https://www.tci-thaijo.org/index.php/APST/index

Published by the Research Department,
Khon Kaen University, Thailand

A comparative study of the structure and morphology of graphene oxide films on glass and aluminum supports by using dip coating

Zamen Karm*

Department of Production Engineering and Metallurgy, University of Technology, Baghdad, Iraq
*Corresponding author: zamen.K.mekhelf@uotechnology.edu.iq

Received 16 December 2023
Revised 30 January 2024
Accepted 1 April 2024

Abstract

In this work, graphene oxide (GO) coating was deposited on glass and aluminum substrates via dip coating. The structural appearance of the coating layer deposited on glass and aluminum substrates was demonstrated using scanning electron microscopy and atomic force microscopy (AFM). Images of the coated substrates were analyzed using ImageJ software. Results show that the probability of distribution can be determined from a histogram of heights measured by AFM. The surface roughness rate of the coated glass and aluminum substrates were compared. In addition, the image software can be successfully used to evaluate starch granule size and shape. The thicknesses of the deposited film were about 0.09 and 0.07 μm for GO coating on aluminum and glass substrates, respectively. The weight loss of the substrates coated with different concentrations of sodium chloride solution under the influence of different times was examined. Results showed that the corrosion rates using the weight loss method for aluminum samples were less than the corrosion rates of coatings on glass substrates.

Keywords: Dip coating, Graphene oxide films, Thickness of film, Weight loss, Corrosion rate

1. Introduction

The field of surface engineering was developed out of the realization that most engineering components could deteriorate or fail catastrophically in service due to surface-related phenomena like wear, corrosion, or fatigue [1]. Typically, coatings are applied to enhance the surface quality of a substrate in terms of wettability, adhesion, and resistance to corrosion. The need to obtain new materials and technologies to increase coating efficiency due to the growing environmental concerns and economic benefits has motivated the coating industry. The quality of the coating, the features of the substrate, the properties of the coating/substrate interface, and the corrosiveness of the surrounding environment are aspects that influence the coating's efficiency against all potential harmful sources [2].

Metals and metal alloys are now essential components of modern life, being used in everything from manufacturing to medical devices, electrical and home goods, transportation, food packaging, housing, and building [3,4]. Aluminum metal and alloys are appealing owing to their high strength-to-weight ratios and their distinctive light weight, high stiffness, and favorable physical characteristics. However, in harsh settings, Al decays and erodes through an electrochemical process that causes wear and energy loss. Numerous methods, including the application of corrosion inhibitors, have been used to protect metals from corrosion because of the enormous economic losses caused by corrosion. Chromium-based coatings have been utilized historically owing to their superior ability to resist corrosion [5,6]. However, their use has recently been discontinued because of growing concerns regarding the environment and safety [6]. In this context, the scientific community has recently become interested in alternative anticorrosion coatings such as those based on silicate minerals [7]. Li et al. [8] demonstrated that adding graphene oxide (GO) may improve the power conversion efficiency of planar heterojunction PVs by suppressing leakage current and reducing recombination through effective hole transport and electron blocking [9]. Although the oxygen groups make GO hydrophilic, they cause low conductivity, suggesting that removing the oxygen groups entirely or in part is necessary to improve the conductivity. In daily

life, glass surfaces are used in many different contexts. Glass is the most popular optical material used for lenses, windshields, solar panels, architectural windows, eye-catching interior and exterior walls, and glass ceilings. In terms of energy-efficient and ecologically friendly building thermal comfort solutions, GO appears as a reasonably priced passive heating and cooling option. With distinct epoxy and hydroxyl groups on the surface, GO has exceptional chemical, optical, and electrical characteristics, enabling it to function as a standalone solar absorber material. Additionally, GO is a more scalable substitute for graphene in large-scale applications [10].

Bai et al. [11] conducted a study on graphene coating and found that even though graphene provides a strong physical barrier that possesses high conductivity; it accelerates the creation of an electrochemical reaction that forms a conductive channel, causing corrosion of the steel surface coating with the zinc (Zn) and epoxy using electroplated (EP). Cui et al. [12] proved that the coating's minor fractures, which quicken local electrochemical corrosion, expose the metal corrosion area and diminish the metal's toughness and strength. This impact has limited its application for graphene as a protective coating for metals. Graphite oxidation produces GO, which possesses a hydrophilic lamellar structure with two dimensions [13]. With its abundance of hydroxyl and epoxy functional groups, including carboxyl and ketone, GO is suitable for organic and inorganic functionalization materials via cross-linking with chemicals [14].

The benefit of dip coating is that it is a low-cost method of solution deposition that is mostly employed to create high-quality thin films and uniformly coat vast regions [15-18]. Therefore, the present study aimed to broaden the understanding and characterization of GO dip coating on two distinct types of substrates: glass and aluminum. ImageJ was utilized to illustrate particle sizing, including the area, perimeter, and shape of particles, for further characterization. The coating's morphology, thickness, and surface roughness were examined. Immersion corrosion techniques were used, and the corrosion rate (mm/y) was calculated for coating glass and aluminum substrates. This investigation revealed that GO is one of the most effective materials for preventing metal corrosion.

2. Materials and methods

2.1 Preparation of coating

Glass and aluminum substrates were used in this work. The glass substrates (10 mm × 10 mm) were cleaned in isopropanol at 50 °C for 20 minutes, acetone at 50 °C for 20 minutes, and then pure water to obtain a surface free of impurities. Aluminum sheets with a 0.5 mm thickness were first cut into squares (10 mm × 10 mm) and then ground using SiC sandpaper. The aluminum samples were cleaned and stripped of natural oxide by immersing them in a 0.5 M sodium chloride (NaCl) solution for 40 seconds at 50 °C, followed by another 40 seconds in a 30% nitric acid (HNO_3) solution. After being cleaned with distilled water, all of the samples were allowed to air dry.

Dip-coating experiments were conducted using a programmable dip coater (Jinlin Ker, China). The substrates were submerged in a 5 mg/mL GO solution for 30 seconds after moving at a speed of 10 mm/min. Afterwards, the substrates were allowed to dry for a whole night in a storage box before going through the characterization process. The GO coatings were examined using scanning electron microscopy (SEM) to determine their morphology and atomic force microscopy (AFM). ImageJ was used to analyze the micrographs to determine the area; perimeter; and shape coefficients, specifically circularity.

2.2 Measurement of the film's thickness

The weight method was employed to determine the thickness of the thin films that were produced. Considering that this approach requires a sensitive electronic balance with four digits only, it can measure the mass of the material that has precipitated on the substrate by dividing the difference between the substrate's mass before (W1) and after thin film deposition (W2). Equation (1) [19] can be used to determine the film's thickness as follows:

$$M(g) = W2-W1 \quad (1)$$

2.3 Measurement of corrosion rate

In the weight loss investigations, the coating specimens were submerged in 1%, 2%, and 3% NaCl solutions at various intervals (24, 48, 72, 96, and 120 hours). Following their removal from the immersion environment, the surfaces of the specimens were cleaned to remove the oxide layer, dried, washed with acetone, and then weighed. The weights of the samples were compared before and after they were exposed to the corrosive media to evaluate the different coatings' levels of corrosion protection. Each weight loss measurement was performed three times to check the repeatability of the data. Equation (2) [20] was used as follows to calculate the corrosion penetration rate (CPR):

$$CPR = \frac{KW}{ADT} \quad (2)$$

where CPR is the corrosion penetration rate (mm/y), D is density (gr/cm^3), T is time (hours), W is weight loss, K is constant K = 87.6 mm/yr, and A is surface area (cm^2).

3. Results and discussion

Figures 1 and 2 show the shape and microstructure of the coating produced from the SEM images. The micrographs show that the graphene coating appears as nanosheets distributed uniformly over the surface. However, GNs are available in a range of sizes because of the polydispersity of graphene.

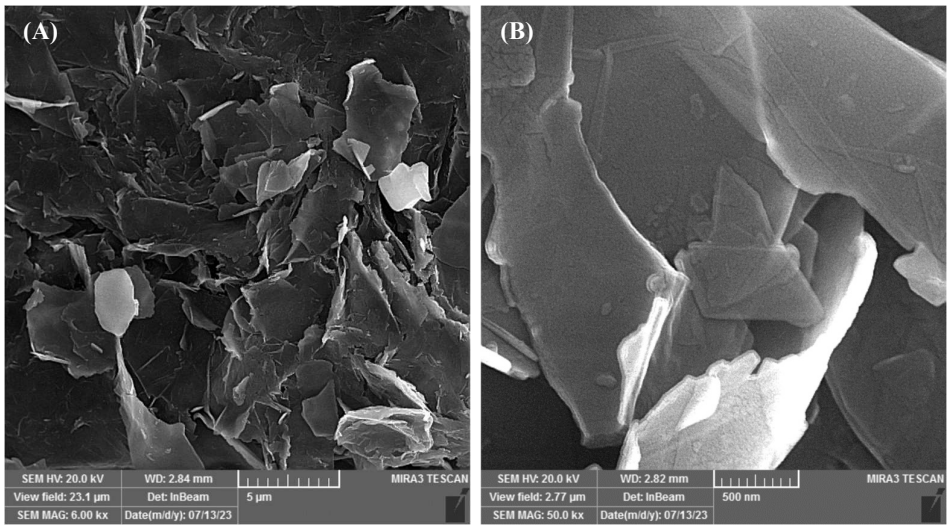

Figure 1 SEM magnification images of GO film on glass substrate at (A) 5 µm and (B) 500 nm.

The morphology of the GO coating on aluminum (Figure 2) was made up of multiple highly wrinkled, thick layers that resemble a structure. The observed flakes were thinner and smaller than the GO coating on glass (Figure 1). Meanwhile, the GO coating on aluminum (Figure 2) was made up of an aggregated flat nanosheet structure (Figure 1) with a somewhat expanded appearance. Figures 1B and 2B clearly show the unique morphology of GO, which is a blocky structure at low magnification and a wrinkled structure at high magnification (Figures 1A and 2A) [21,22]. At low magnification, several free-standing sheets that resembled the shape of GO are shown in Figures 1B and 2B. The GO flakes created regions of brightness that were darker than the background of the bare substrate.

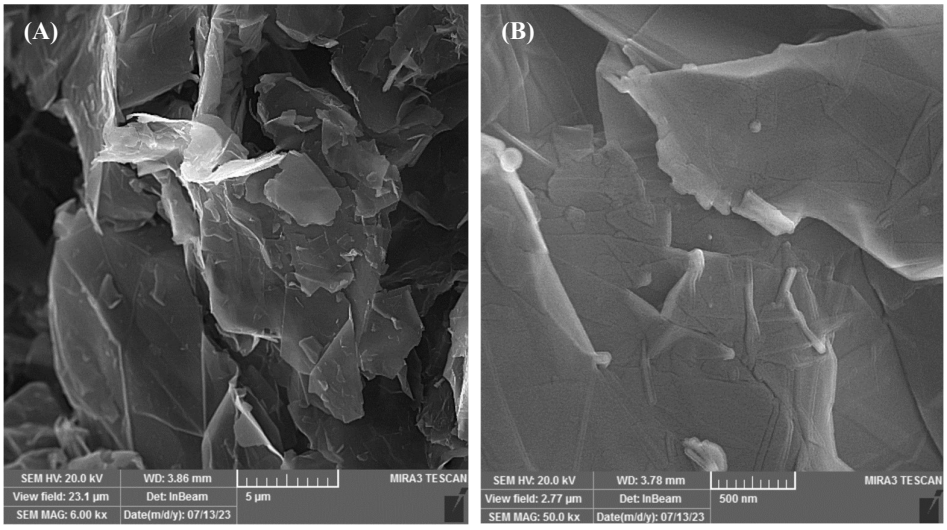

Figure 2 SEM magnification images of GO film on aluminum substrate at (A) 5 µm and (B) 500 nm.

The coating on an aluminum substrate was flatter than on a glass substrate, as shown by the SEM images in Figures 1 and 2, causing the layer deposited on the aluminum substrate to thicken.

The thickness values of coatings on glass and aluminum substrates were 0.07 and 0.09 µm, respectively, which were calculated using Equation (1), indicating that the film thickness increased with increasing roughness and hydrophobic characteristics for substrates. The results are consistent with the AFM results, which showed that the aluminum substrate was rougher than the glass substrate [23].

Regarding coating GO on glass and aluminum substrates, the findings of ImageJ processing of the photos (Table 1) indicate that coating GO on glass was the largest and coating GO on aluminum substrate was the smallest. The shape factors represented by circularity measures were 0.111 and 0.458 for coating GO on aluminum and glass substrates, respectively.

Table 1 Measurement parameters for coating substrates.

Substrate	Average size (µm)	%Area	Perim. (µm)	Circ.
Glass	38.425	25.391	45.612	0.111
Aluminum	5.839	3.166	14.096	0.458

The 2D and 3D AFM images in Figures 3 and 4 provide information about the roughness of the surface of the coating substrates. Figure 4 and Table 2 exhibit the values of root mean square (RMS) and average roughness (Ra). The values of RMS and Ra for coating the glass substrate were 599.2 and 464.5 nm, respectively, and those for coating the aluminum substrate were 755.8 and 594.6 nm, respectively. The observed increase in RMS roughness for coating aluminum substrates over glass substrates was due to the fact that the coating layer on the aluminum substrate is thicker than on the glass substrate.

The roughness coating of the aluminum substrate was higher than that of coating the glass substrate, as shown in the SEM image, and this finding was confirmed by the subsequent AFM examination. GO particles accumulated on the aluminum substrate; therefore, the coating layer was very rough, and the coating particles were oriented for coating aluminum. In addition, when the coating density increased, the molecules became more closely linked and more uniform, leading to increased coating coverage, and consequently, the thickness of the coating layer increased, as is the case when coating aluminum.

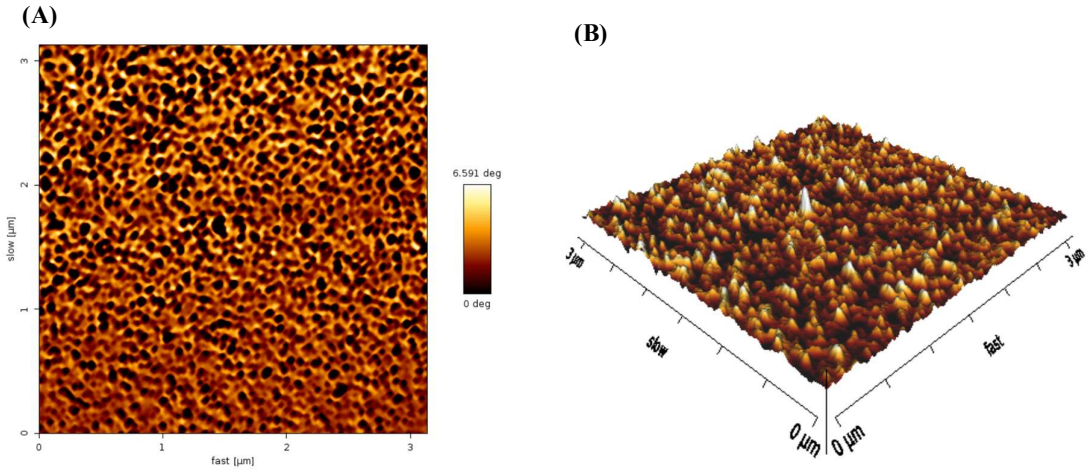

Figure 3 Atomic force microscopy of composite adsorbent material; (A) two-dimensional and (B) three-dimensional distribution.

The increase in RMS roughness for coating aluminum substrates over glass substrates is due to the fact that the coating layer on the aluminum substrate is thicker than on the glass substrate.

The results from Figures 3 and 4 and Table 2 show that the average roughness coating of GO on glass was the lowest, and that of GO on aluminum was the lowest, indicating that the GO on aluminum had the most obvious wrinkle. Another clear conclusion is that the surface roughness of the glass was smoother, and therefore, the deposited layer was smoother than that of the aluminum substrate. These results were confirmed by SEM examinations.

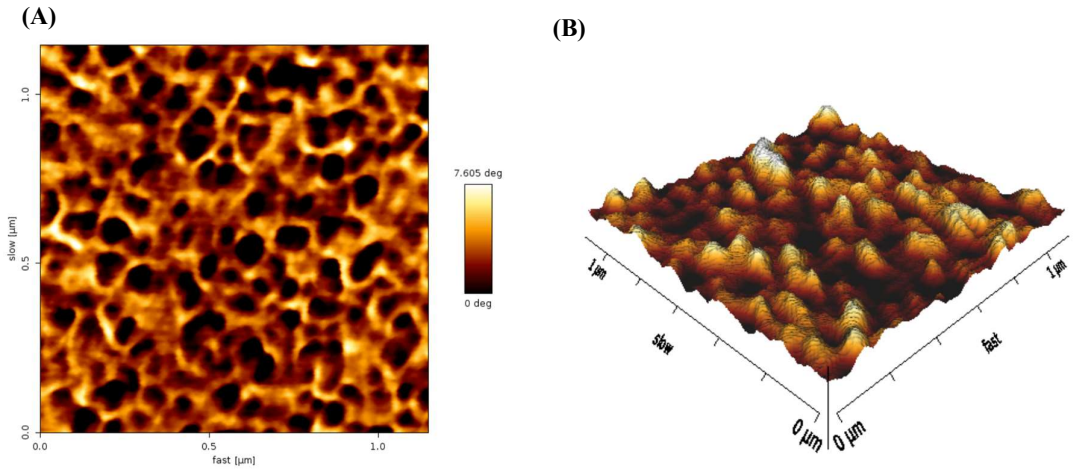

Figure 4 Atomic force microscopy of composite adsorbent material: (A) two-dimensional and (B) three-dimensional distributions.

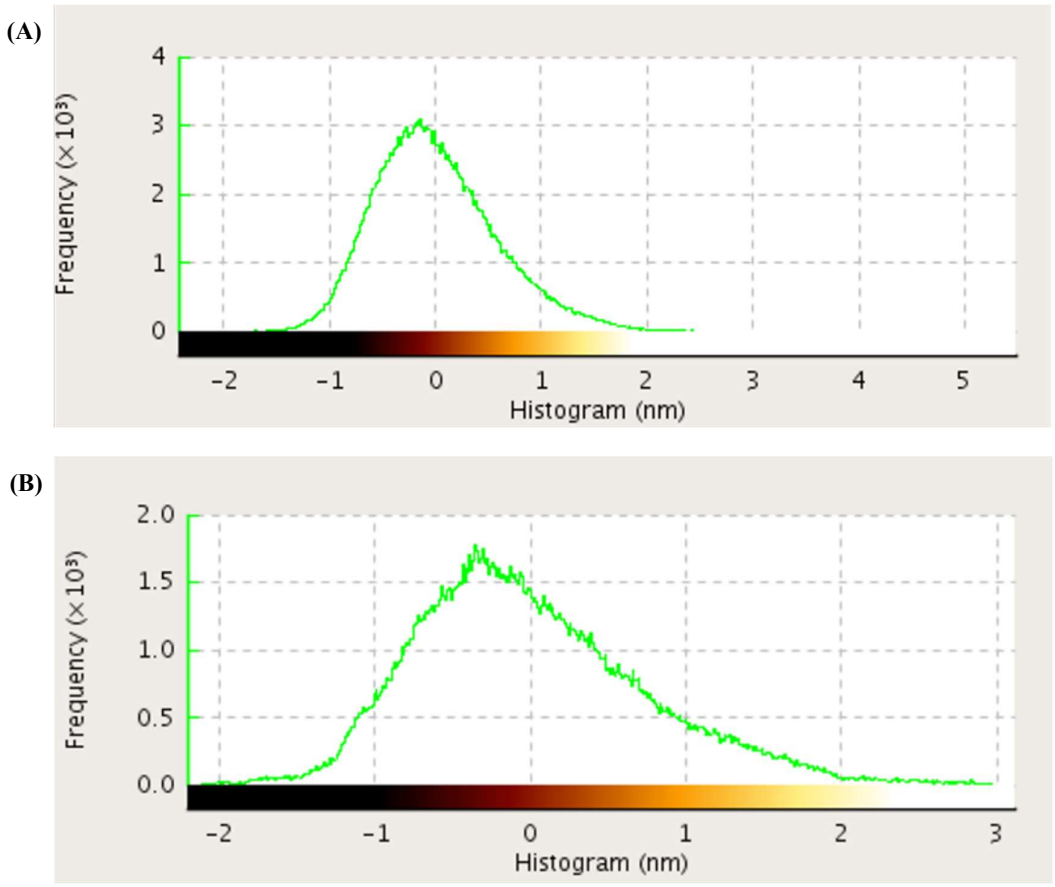

Figure 5 Histogram of surface height coating of (A) glass substrate and (B) aluminum substrate.

Table 2 AFM of surface roughness GO on glass and aluminum substrates.

Substrate	Ra (nm)	Root mean square (rms)
Glass	464.5	599.2
Aluminum	594.6	755.8

The substrates were weighed after being immersed in 1%, 2%, and 3% NaCl solutions for 24, 48, 72, 96, and 120 hours. As shown in Figures 6–8, the concentration of chloride ions affected the coating layer's corrosion rates. The results of the immersion method show that the coating of GO on glass substrates displayed the largest corrosion rate decrease when compared with the coated aluminum substrate, which showed the least in the substrate. In addition, the greater the contact time between the samples and the corrosion solution, the greater the corrosion rate of the substrate of the samples. These results are consistent with [24]. In addition, increasing the concentrations of chloride ions can cause an increase in the corrosion rates on the coating layers on substrates. When the concentration of Cl^- increased, the coatings showed an increase in corrosion rate. In this work, the corrosion rate in solutions with greater concentrations was significantly more impacted by changes in Cl^- concentration than in solutions with lower concentrations. If the corrosive intermediate (Cl) was present in higher amounts in the NaCl solution, it could expeditiously permeate the outer layer and arrive at the surface of the specimen. As a result, the rate of corrosion increased. These results were in agreement with those of [25,26].

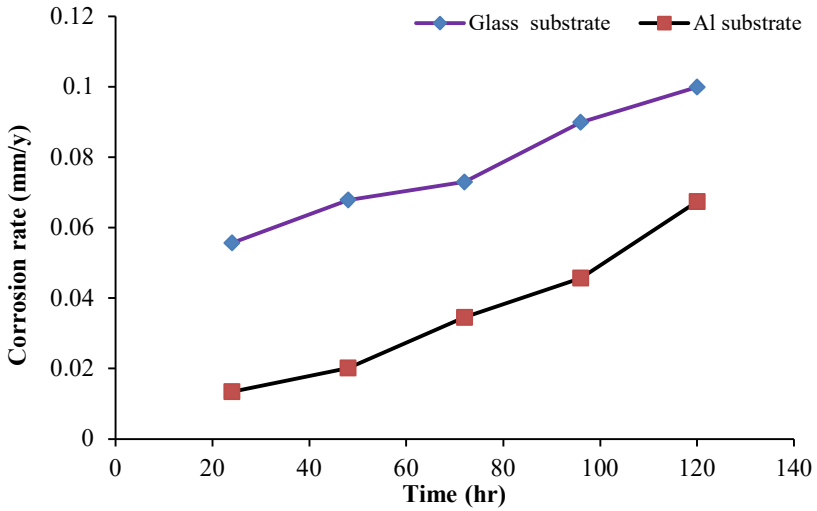

Figure 6 Varying corrosion rate (mm/y) against immersion time for aluminum and glass substrates in 1% NaCl solution.

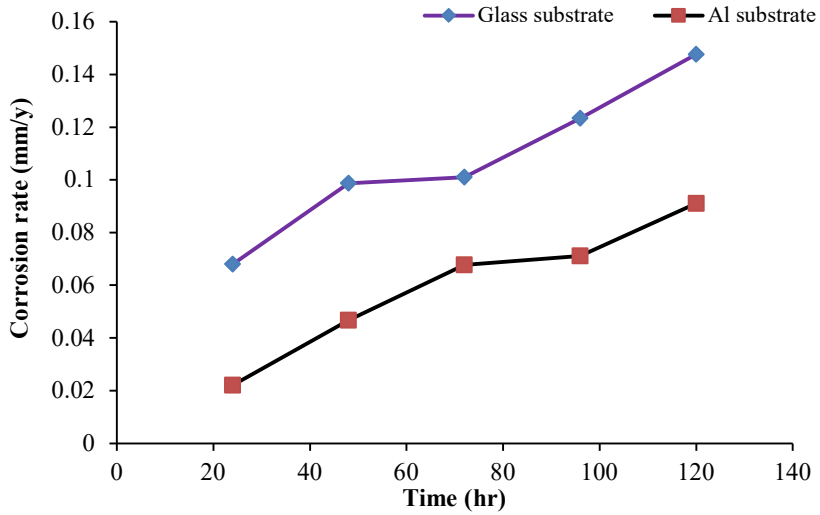

Figure 7 Varying corrosion rate (mm/y) against immersion time for aluminum and glass substrates with 2% NaCl solution.

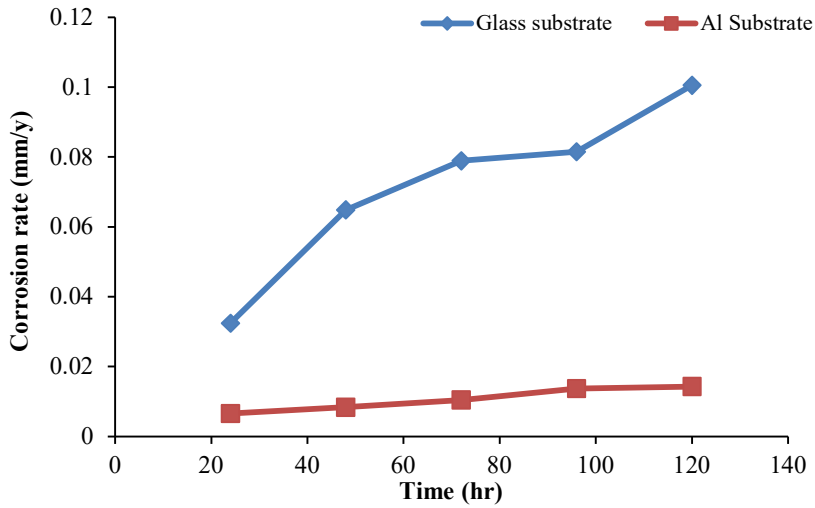

Figure 8 Varying corrosion rate (mm/y) against immersion time for aluminum and glass substrates with 3% NaCl solution.

4. Conclusion

The coating of GO was experimentally investigated using dip coating on two different substrates made of aluminum and glass. AFM and SEM were employed to evaluate the quality of coatings created from GO flakes. The results of measuring the thickness and roughness of the coatings deposited on the aluminum surface were higher than those on the glass substrate. An image analysis tool was used to compare the GO coatings on these samples. The results demonstrated that more coating was deposited on the aluminum surface, and the shape factor was higher for aluminum than for glass substrate. The weight loss of coating an aluminum substrate in a solution for different periods of time (24, 48, 72, 96, and 120 hours) and sodium chloride concentrations was less than that of coating an glass substrate.

5. Conflict of Interests

There is no conflict of interest.

6. References

[1] Song GL, Feng Z. Modification, degradation and evaluation of a few organic coatings for some marine applications. Corros Mater Degrad. 2020;1(3):408-442.

[2] Sun X, Huang C, Wang L, Liang L, Cheng Y, Fei W, Li Y. Recent progress in graphene/polymernanocomposites. Adv. Mater. 2020;33(6):2001105.

[3] Zhao J, Xia L, Sehgal A, Lu D, McCreery R.L, Frankel GS. Effects of chromate and chromate conversion coatings on corrosion of aluminum alloy 2024-T_3. Surf Coatings Technol. 2001;140(1):51-57.

[4] Clark WJ, Ramsey JD, McCreery RL, Frankel GS.A Galvanic corrosion approach to investigating chromate effects on aluminum alloy 2024-T_3. J Electrochem Soc. 2002;149(5):51-57.

[5] Pellerin C,Booker SM, Reflections on hexavalent chromium: health hazards of an industrial heavy weight. Environ Health Perspect, 2000;108(9):A402-A407.

[6] Gibb HJ, Lees PS, Pinsky PF,Rooney BC. Lung cancer among workers in chromium chemical production. Am J Ind Med. 2000;38(2):115-126.

[7] Wood JW, Beecher JS, Laurence PS. Some experiences with sodium silicate as a corrosion inhibitor in industrial cooling waters. Corrosion. 1957;13(11):41-46.

[8] Li D, Cui J, Li H, Huang D, Wang M, Shen Y. Graphene oxide modified hole transport layer for $CH_3NH_3PBI_3$ planar heterojunction solar cells. Sol Energy. 2016;131:176-182.

[9] Chen L, Zhang Y, Wu Q . Effect of graphene coating on the heat transfer performance of a composite anti-/deicing component. Coatings. 2017;7(10):158.

[10] Sriram S, Singh RK, Kumar A. Silica and silane based polymer composite coating on glass slide by dip-coating method. Surf Interfaces. 2020;19:100472.

[11] Bai W, MaY, Meng M, Li Y. The influence of graphene on the cathodic protection performance of zinc-rich epoxy coatings. Prog Org Coat. 2021;161:106456.

[12] Bohm S. Graphene against corrosion. Nature Nanotech. 2014;9:741-742.
[13] Cui C, Lim ATO, Huang. A cautionary note on graphene anti-corrosion coatings. Nat Nanotechnol. 2017; 12(9):834-835.
[14] Kim J, Cote LJ, Kim F, Yuan W, Shull KR, Huang J. Graphene oxide sheets at interfaces. J Am Chem Soc. 2010;132(23):8180-8186.
[15] Majumder P, Gangopadhyay R. Evolution of Graphene Oxide (GO)-based nanohybrid materials with diverse compositions: an overview. RSC Adv. 2022;12(9):5686-5719.
[16] Dreyer DR, Park S, Bielawski CW, Ruoff RS. The chemistry of graphene oxide. Chem Soc Rev. 2010; 39(1): 228-240.
[17] Yu Z, Di H, Ma Y, He Y, Liang L, Lv L, Ran X, Pan Y, Luo Z. Preparation of graphene oxide modified by titanium dioxide to enhance the anti-corrosion performance of epoxy coatings. Surf Coat Technol. 2015;276: 471-478.
[18] Yan Y, Liu J, Zhang B, Xia R, Zhang Y, Guan Z. Enhanced mechanical and hydrophobic antireflective nanocoatings fabricated on polycarbonate substrates by combined treatment of water and HMDS vapor. Materials. 2023;16(10):3850.
[19] Mohamed L, Hamdy G, Gaber G. Performance of GO/SiO_2, GO/TiO_2, and GO/ZrO_2 nanocomposites coatings as a corrosion barrier layer on Al-Si-Cu-mg alloy in 3.5% NaCl solution. Int J Electrochem Sci. 2021;16(5): 210515.
[20] Abdul Hussein AM, Abdullah SA, Rasheed M, Zamel RS. Optical and electrical properties of glass/graphene oxide thin films. Iraqi Journal of Physics. 2020;18(47):73-83.
[21] Tjahjanti P, Firdaus R, Iswanto, Irfian A. Corrosion protection of low carbon steel by coating of graphene oxide nanoparticles and galvanization process. J Nanostruct. 2022;12(1):20-27.
[22] Dhawade P, Jagtap R. Comparative study of physical and thermal properties of chitosan-silica hybrid coatings prepared by sol–gel method. Chem Sin. 2012;3(3):589-601.
[23] Yang Y, Rigdon W, Huang X, Li X. Enhancing graphene reinforcing potential in composites by hydrogen passivation induced dispersion. Sci Rep. 2013;3(1):2086
[24] Mahdi BR, Al.mamori AF, Mahdi AM .Synthesis of nano-TiO_2 thin films by sol-gel dip-coating method. Eng. &Tech.Journal.2015;33(7B):1303-1312.
[25] Wang Q, Yan T, Ding L. Effect of Seawater environment on the structure and performance of basalt continuous fiber. Materials. 2021;14(8):1862.
[26] Thirumalaikumarasamy D,Shanmuga K, Balasubramanian V. Influence of chloride ion concentration on immersion corrosion behaviour of plasma sprayed alumina coatings on AZ31B magnesium alloy. J Magnes Alloy. 2014;2(4):325-334.